

Single top production at the LHC: the Effective W Approximation*

D. Espriu[†] and J. Manzano[‡]

Departament d'Estructura i Constituents
de la Matèria and IFAE,
Universitat de Barcelona,
Diagonal, 647, E-08028 Barcelona

Abstract

Motivated by the need to set bounds on the third generation charged couplings, we study the mechanism of single top production at the LHC, analyzing the sensitivity of different observables to the magnitude of the effective left and right couplings. The study is carried out in the framework of the so-called effective W approximation, where the virtual W is treated as a parton. We take this opportunity to critically assess the validity of this approximation in detail by comparing it to an exact calculation recently completed by us of the same process. We comment on several issues related to top polarization since the observables relevant to distinguish between left and right effective couplings involve the measurement of the spin of the top. The conclusion is that the effective W approximation is not well suited for this subtle analysis; it fails to reproduce the detailed p_T distributions and grossly distorts the polarization of the emerging top. It does however, reproduce the overall angular distribution and gives a sensible order-of-magnitude estimate for the total cross section analysis.

UB-ECM-PF 01/09

August 2001

*Contribution presented in the XXIX International Meeting on Fundamental Physics, Sitges, February 2001. Dedicated to F.J.Ynduráin on his 60th birthday.

[†]espriu@ecm.ub.es

[‡]manzano@ecm.ub.es

1 Introduction

The main purpose of this work is to analyze the applicability of the so-called effective- W approximation (to be described below) to the study of single top production at the LHC, the aim being to set bounds on the effective couplings for the charged couplings involving the third generation.

It is quite conceivable that the Standard Model should be considered as an effective theory valid only at low energies ($\lesssim 1$ TeV). In particular, since the Higgs particle has not been observed yet (the current bound on the Standard Model Higgs is at 113.5 GeV [1]), it makes sense to consider as an alternative to the minimal Standard Model an effective theory without any physical light scalar fields. Alternatively, it may well be that the Higgs particle, or, as a matter of fact, any other scalars, which abound in extensions of the minimal Standard Model, are much heavier than the weak scale, granting an expansion in inverse powers of such heavy masses. How heavy must the Higgs particle—or the scale associated to new physics, for that matter— be for such an expansion to be useful? In practice, 300 or 400 GeV are sufficient for the expansion to be useful at the M_Z scale, as detailed calculations[2] show. In a process like the one we shall discuss in this paper, where the individual energies involved are typically peaked in the 200 - 400 region, the momentum expansion should be appropriate provided that the relevant scale for the new physics is in the 1 TeV region or beyond. While admittedly this is not the scenario favoured by the comparison with the electroweak data[3], it cannot be properly excluded until a (relatively) light elementary Higgs is found.

In the effective lagrangian, only the light (respect to the energies of the process) degrees of freedom are kept, while the information about the heavier degrees of freedom is contained in an infinite set of effective operators of increasing dimensionality, compatible with the electroweak and strong symmetries $SU(3)_c \times SU(2)_L \times U(1)_Y$. The coefficients of these operators would parametrize different choices of new physics beyond the Standard Model. In this framework [4] one can describe the low energy physics of theories exhibiting the pattern of symmetry breaking $SU(2)_L \times U(1)_Y \rightarrow U(1)_{em}$. Both global and gauge symmetries are non-linearly realized and the effective theory is non-renormalizable (the Higgs field, which is absent here, is a necessary ingredient both for the linear realization and renormalizability of the minimal Standard Model). The additional operators serve thus a dual purpose; on the one hand they encode low-energy effects of the so-far unexplored high-energy scales. On the other hand, these operators are necessary as counterterms to absorb ultraviolet divergences generated by quantum corrections from the lower dimensional (universal) terms.

In this work we are concerned about the new features that physics beyond the Standard Model may introduce in the production of single top quarks through W -gluon fusion at

the LHC. We are interested only in the leading non-universal (i.e. not appearing in the standard model at tree level) effective operators in the low energy expansion. In the present context these correspond to those operators of dimension four, which were first classified by Appelquist et al. [5]. These operators are characteristic of strongly coupled theories (i.e. of theories without an elementary Higgs or a very heavy one) and require a non-linear realization of the gauge symmetry. Therefore they are absent in the minimal Standard Model and in modifications thereof containing only light fields. When one particularizes to the W interactions, for instance by going to the unitary gauge, these operators induce effective fermion-gauge boson couplings, and these effective couplings are the object of our interest.

Of course radiative corrections induce form factors in the vertices too. Assuming a smooth dependence in the external momenta these form factors can be expanded and at leading order in the derivative expansion they just induce effective fermion-gauge boson effective couplings, exactly as the putative contribution from new physics. These radiative corrections are typically very small, at the few per cent level, but in general non-negligible (particularly those involving the top mass). Obviously any deviation from the values of these couplings with respect to the values predicted by the minimal Standard Model would indicate the presence of new physics in the matter sector. The extent to which a machine like the LHC can set direct bounds on these couplings, in particular on those involving the third generation, is thus of obvious interest.

In fact there if anywhere are deviations with respect to the Standard Model to show up in the matter sector, this is the place to look for them. Many alternatives to the minimal Standard Model (dynamical symmetry breaking models, for instance) predict large deviations for the third generation effective couplings in a natural way (typically much larger than radiative corrections from the minimal Standard Model itself). The fact that the longitudinal degrees of freedom of the vector bosons—the very product of the electroweak symmetry breaking—have couplings that, after use of the equations of motion, are proportional to the quark masses hint in this same direction too. For all these reasons we regard the possibility of getting a handle on such effective couplings as one of the main tasks of the LHC experiments.

2 Top Production at the LHC

Let us now briefly review the mechanisms of top production. At the LHC energy (14 TeV) the dominant mechanism for creating tops is gluon-gluon fusion. This is a purely QCD process, its total cross-section is 800 pb[6]. It is obvious that tops will be copiously produced at the LHC and that a lot can be learned by a detailed analysis of their decays, for instance. We note, however, that this mechanism of production has nothing to do with the electroweak

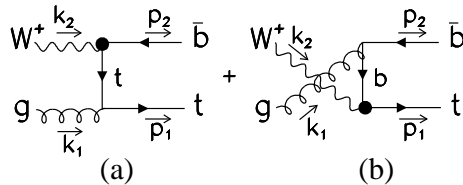


Figure 1: Feynman diagrams contributing to the single top production subprocess

sector and thus is not the most adequate for our purposes. In fact, since colour symmetry, like electromagnetism, is unbroken, the form factor is unchanged at the lowest order in the derivative expansion and new physics cannot possibly affect this effective coupling at the order we are working [7]. In addition, we shall not be interested here in top decay, but rather in how new physics can affect the way top (or anti-top) are produced at the LHC. For these reasons, the dominant mechanism of top production at the LHC is not interesting at all for our purposes, and for us it will just be a background to worry about.

At tree level, electroweak physics enters the game through single top production. (For a recent review see e.g. [8].) At LHC energies the (by far) dominant electroweak subprocess contributing to single top production is given by a gluon (g) coming from one proton and a positively charged W^+ coming from the other (this process is also called t -channel production[9, 10]). This process is depicted in diagrams (a) and (b) of Fig.1. The total cross section for this process at the LHC is 250 pb, to be compared to 50 pb for the associated production¹ with a W^+ boson and a b -quark extracted from the sea of the proton, and the 10 pb corresponding to quark-quark fusion (s -channel production). For a detailed discussion see [10]. For comparison, at the Tevatron (2 GeV) the cross section for W -gluon fusion is 2.5 pb, so the production of tops through this particular subprocess is really copious at the LHC. Monte Carlo simulations including the analysis of the top decay products indicate that this process can be analyzed in detail at the LHC and traditionally has been regarded as the most important one for our purposes.

In a proton-proton collision a bottom-anti-top pair is also produced, through the subprocesses (a) and (b) of Fig.2. However, these subprocesses are suppressed roughly by a factor of two (see Fig.6) because the proton has much lesser probability of emitting a W^- than emitting a W^+ , and at any rate qualitative results are very similar to those corresponding to the subprocess of Fig.1, from where the cross sections can be easily derived doing the appropriate changes.

Thus, even if subdominant, single top production through an electroweak vertex is not

¹the difference between the two processes is purely kinematic; see section 5. The above values correspond to the cuts used in [10]

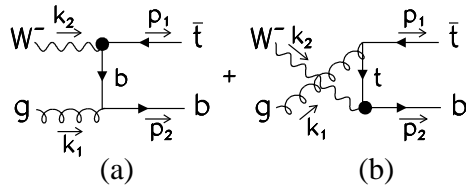


Figure 2: Feynman diagrams contributing to the single anti-top production subprocess

negligible at all; more than one third of all tops or anti-tops that will be produced at the LHC will be created through this mechanism. Furthermore, this mechanism has rather distinctive kinematics, as we shall see in this work. Indeed, single top production, being dominated by the exchange of a massless (by comparison to the energies involved) particle in the t channel, is strongly peaked in the beam direction, with a characteristic angular distribution (see below).

Several analysis of top production exist in the literature. A (surely incomplete) list of the references we have used is given in [8, 9, 10] and [11, 12]. The second group of references is mostly concerned with the issue of the top polarization. Indeed, since the top decays shortly after production, much before strong effects can set in, the decaying products (a b quark and a W , which, in turn, decays into e.g. a charged lepton and a neutrino) carry information about the spin of the top. In particular, if the top is in a pure state of spin (and hence being a $s = 1/2$ fermion its polarization vector points in the top rest frame in a particular direction in space), the decaying lepton has an angular distribution peaked in the direction where the top polarization vector is pointing to.

So far the issue as to what extend LHC can set bounds on the top-bottom effective couplings has not been analyzed in much detail in the literature. In the effective lagrangian language, the contribution from operators of dimension five to top production via longitudinal vector boson fusion was estimated some time ago in [13], although the study was by no means complete. It should be mentioned that t, \bar{t} pair production through this mechanism is very much masked by the dominant mechanism of gluon-gluon fusion, while single top production, through WZ fusion, is expected to be quite suppressed compared to the mechanism presented in this paper, the reason being that both vertices are electroweak in the process discussed in [13], and that operators of dimension five are expected to be suppressed, at least at moderate energies, such as the ones that in practice count at LHC, by some large mass scale. The effects due to anomalous couplings introduced through operators of dimension six have been recently analyzed in [14]. All the contributions from higher dimensional operators are expected in realistic models to be small and far beyond the sensitivity of LHC. For these reasons we concentrate only on dimension four operators. In practice this means bounds on

the left and right top effective couplings (see also [15]) thus providing further reasons for a good measurement of these parameters.

The potential for single top production for measuring the CKM matrix element V_{tb} , and hence the top-bottom effective left coupling has certainly been previously studied (see e.g. [9], [10] and our recent work [16]), but drawing firm conclusions requires a good knowledge of the total normalization of the cross-section, something which is very influenced by issues on which a good theoretical control is problematic, such as the QCD scale. Next to leading calculations such as the ones presented in [17, 18] for the total cross section are mandatory but results still leave an uncertainty at the 5% level, so this will be the final level of uncertainty on the left effective coupling. Nothing is known on bounds on the right effective couplings. On the other hand, it is clear that this is a very urgent issue. The only noticeable discrepancy of the whole of the LEP results when compared to the minimal Standard Model lies in the bottom effective couplings (actually on the right coupling). Our original motivation for this work was to partly fill in this gap. This looks feasible with machines like the LHC which are efficient top factories.

3 Effective Couplings

The alert reader may have noticed in the previous paragraphs that we attach a lot of importance to the contribution of dimension four operators —they may encode the larger contribution in a large family of extensions of the Standard Model.

On the other hand, it is sometimes stated that gauge invariance prevents the presence of dimension four operators other than the ones already existing in the Standard Model, thus forcing the contribution of new physics to be suppressed by powers or otherwise renormalizing the gauge coupling constant. This widespread belief is not correct when the symmetry is non-linearly realized. The complete set of dimension four effective operators (which may eventually contribute to the top effective couplings) is [5, 19]

$$\begin{aligned}
\mathcal{L}_4^1 &= i\delta_1 \bar{f} \gamma^\mu U (D_\mu U)^\dagger Lf, & \mathcal{L}_4^2 &= i\delta_2 \bar{f} \gamma^\mu U^\dagger (D_\mu U) Rf, \\
\mathcal{L}_4^3 &= i\delta_3 \bar{f} \gamma^\mu (D_\mu U) \tau^3 U^\dagger Lf + h.c., & \mathcal{L}_4^5 &= i\delta_5 \bar{f} \gamma^\mu \tau^3 U^\dagger (D_\mu U) Rf + h.c., \\
\mathcal{L}_4^4 &= i\delta_4 \bar{f} \gamma^\mu U \tau^3 U^\dagger (D_\mu U) \tau^3 U^\dagger Lf, & \mathcal{L}_4^6 &= i\delta_6 \bar{f} \gamma^\mu \tau^3 U^\dagger (D_\mu U) \tau^3 Rf, \\
\mathcal{L}_4^7 &= i\delta_7 \bar{f} \gamma^\mu U \tau^3 U^\dagger D_\mu^L Lf + h.c., & &
\end{aligned}$$

where $L = \frac{1-\gamma^5}{2}$, $R = \frac{1+\gamma^5}{2}$ are the left and right projectors. The matrix-valued field $U(x)$ is an $SU(2)$ matrix containing the three Goldstone bosons associated to the spontaneous breaking of the symmetry. The covariant derivatives appearing in the above operators are

$$D_\mu U = \partial_\mu U + ig \frac{\boldsymbol{\tau}}{2} \cdot \mathbf{W}_\mu U - ig' U \frac{\tau^3}{2} B_\mu,$$

Vertex	Feynman Rule
$\bar{t}gt$	$-ig_s \frac{\lambda^a}{2} \gamma_\mu (1 + 2\delta_7 L)$
$\bar{b}gb$	$-ig_s \frac{\lambda^a}{2} \gamma_\mu (1 - 2\delta_7 L)$
$\bar{t}W^+b$	$-\frac{i}{\sqrt{2}}g\gamma_\mu (g_L L + g_R R)$
$\bar{b}W^-t$	$-\frac{i}{\sqrt{2}}g\gamma_\mu (g_L^* L + g_R^* R)$

Table 1: Feynman rules for the vertices appearing in the subprocesses of Figs.(1) and (2).

$$\begin{aligned}
D_\mu^L f &= \left(\partial_\mu + ig \frac{\boldsymbol{\tau}}{2} \cdot \mathbf{W}_\mu + ig' \frac{1}{6} B_\mu + ig_s \frac{\boldsymbol{\lambda}}{2} \cdot \mathbf{G}_\mu \right) f, \\
D_\mu^R f &= \left(\partial_\mu + i \frac{g'}{2} \left(\tau^3 + \frac{1}{3} \right) B_\mu + ig_s \frac{\boldsymbol{\lambda}}{2} \cdot \mathbf{G}_\mu \right) f.
\end{aligned}$$

Finally, f is a weak doublet of matter fields ((t, b) in our case). Generation mixing has been neglected. The above operators contribute to the different gauge boson-fermion-fermion vertices as indicated in table 1.

In addition, the operator \mathcal{L}_4^7 also contributes to the quark self energies and to the counterterms required to guarantee the on-shell renormalization conditions [19], but when we take into account all these contributions, δ_7 vanish from the observables in the present case. It should be noted, however, that the internal quark line in the diagrams in Figs.(1) and (2) are never on-shell and the use of the equations of motion to eliminate \mathcal{L}_4^7 , is a priori not justified. The net effect of the electroweak effective lagrangian in the charged current sector can thus be summarized, to the order we have considered, in the effective couplings g_L and g_R .

$$g_L = 1 + \delta g_L = 1 - (\delta_1 + \delta_4) \quad g_R = \delta g_R = \delta_2 - \delta_6. \quad (1)$$

At present not much is known from direct measurements for the $t \rightarrow b$ effective coupling. This is perhaps best evidenced by the fact that the current experimental results for the (left-handed) V_{tb} matrix element give [20]

$$\frac{|V_{tb}|^2}{|V_{td}|^2 + |V_{ts}|^2 + |V_{tb}|^2} = 0.94_{-0.24}^{+0.31}. \quad (2)$$

It should be emphasized that these are the ‘measured’ or ‘effective’ values of the CKM matrix elements, and that they do not necessarily correspond, even in the Standard Model, to the entries of a unitary matrix on account of the presence of radiative corrections, even though these deviations with respect to unitarity are expected to be small unless new physics is present. At the Tevatron, it is said, the left-handed couplings are expected to be eventually measured with a 5% accuracy [21], but as mentioned above this depends on absolute scale normalizations which are hard to pin down, even after a full two-loop QCD calculation.

As far as experimental bounds for the right handed effective couplings is concerned no direct relevant bounds exist, the more stringent ones are indirect and come from the measurements on the $b \rightarrow s\gamma$ decay at CLEO [22]. Due to a m_t/m_b enhancement of the chirality flipping contribution, a particular combination of mixing angles and κ_R^{CC} can be found. The authors of [23] reach the conclusion that $|\text{Re}(\kappa_R^{CC})| \leq 0.4 \times 10^{-2}$. However, considering κ_R^{CC} as a matrix in generation space, this bound only constraints the tb element. Other effective couplings involving the top remain virtually unrestricted from the data. Nonetheless the previous bound on the right-handed coupling is a very stringent one. It is fairly clear that an hadron machine such as the LHC will never be able to compete with such a precision. Yet, the measurement would be a direct one, not through loop corrections. Equally important is that it will yield information on the ts and td elements too, by just replacing the quark exchanged in the t -channel in Fig.1 (b).

4 The effective- W approximation

The calculations presented in this work are carried out in the framework of the so-called effective- W approximation that is the translation to the present case of the familiar Weiszäcker-Williams[24] approximation for photons.

Known to be accurate at high energies (see e.g. [25] for a discussion on accuracy and improvements) and very convenient, this approach is computationally simple and has all the attractive physical interpretation of the parton model. One certainly would expect that the translation of the Weiszäcker-Williams approximation to W 's is a good one at sufficiently high energies. In LHC physics it has been amply used in the context of WW , WZ or $W\gamma$ scattering. (See e.g. [26] for a very recent application and references.) In [28], the author claims without much elaboration that the approximation works well for colliders at 20 TeV or higher energy. LHC falls somewhat short of this energy, so the applicability becomes a bit problematic. This has motivated us to look into this question in somewhat more detail. We shall later discuss to what extent the above expectations are fulfilled.

In this work the production of polarized tops is considered. As we shall see in the appendix, within the frame of the effective- W approximation this is absolutely necessary if one wishes to set bounds on the right-handed effective couplings. In doing so we have found results which are somewhat at variance with the recent work reported in [11]. A priori it would not be clear whether the difference can be blamed on the effective- W approximation itself or in the use of different kinematical cuts (which in turn are somewhat forced upon us by the same effective- W approximation). Because of this, we shall review in the coming pages not just total cross sections but cross sections for the production of polarized tops and quite

detailed p_T and angular distributions and compare the results obtained using the effective- W approximation to the ones of the exact calculation [16] we performed recently.

In order to calculate the cross section of the process $pp \rightarrow t\bar{b}$ we have used the CTEQ4 structure functions [27] to determine the probability of extracting a parton with a given fraction of momenta from the proton. The u and d -type partons then radiate a W^- or W^+ boson, respectively.

In the effective- W approximation these W bosons (both longitudinal and transverse) are treated as partons from the proton, carrying a fraction of the quark momentum and thus of the momentum of the proton. The W parton distribution function is, roughly speaking, the probability of producing a W with such a fraction of the momentum. In the spirit of the Weizsäcker-Williams approximation, the cross-section for the process $pp \rightarrow t\bar{b}X$ (for instance) is approximated by the product of cross sections

$$\int_0^1 dy \int_0^1 d\hat{x} \int d^2k_T d^2k'_T \sigma(pp \rightarrow W(k)g(k')) \left(\frac{1}{k'^2}\right)^2 \left(\frac{1}{k^2 - M_W^2}\right)^2 \hat{\sigma}(k, k'), \quad (3)$$

where $\hat{\sigma}$ is the physical cross-section for the subprocess; $Wg \rightarrow t\bar{b}$ in our case. In this subprocess cross section, both the W and the gluon are assumed to be on-shell, i.e. we have a physical, gauge independent, cross section. Of course the W is never on-shell. Kinematically, the W has a space-like four momentum, and it is off its mass shell by an amount which is, at least, M_W^2 . However, at the energies which are characteristic of the LHC, one expects the error to be small. The variables \hat{x} and y are the fractions of the proton energy carried by the W and gluon, respectively. k_T and k'_T are the respective transverse momenta of W and gluon. Hereafter when we talk about components of a given four-momentum we consider them given in the LAB frame (center-of-mass frame of the two protons). The W momentum can be written as $k = (\hat{x}E, k_T, \omega)$, where ω is the longitudinal momentum of the W , E is the energy of the u parton, and \hat{x} the fraction of the parton energy carried by the W . E is related to the total energy of the proton by $E = xE_P$, E_P being the proton energy in the LAB frame.

Energy-momentum conservation in the vertex requires that, if the emerging ‘spectator’ quark (a d quark if the parton radiating the W is a u quark) is to be on-shell, the squared four-momentum of the W is negative or zero. In this case, $\omega = E - \sqrt{(1 - \hat{x})^2 E^2 - k_T^2}$, and the cut for the integration over k_T is, of course, $(1 - \hat{x})E$. The W is off-shell by at least an amount M_W^2 . On the other hand, one may decide to set the W on-shell, since the subprocess cross-section is after all computed for on-shell W ’s (and only in this case it is physically meaningful and gauge independent). In this case, the longitudinal momentum carried by the W is $\omega = \sqrt{\hat{x}^2 E^2 - M_W^2 - k_T^2}$, and the cut on the integration over transverse momenta will be $\sqrt{\hat{x}^2 E^2 - M_W^2}$. This latter choice sets the ‘spectator’ quark off-shell by a virtuality of

order M_W^2 (recall that previously it was the W itself which was off-shell).

In either case, we rewrite Eq.(3) in the form

$$\int_0^1 dy f_g(y) \int_0^1 dx f_u(x) \int_0^1 d\hat{x} f_W(\hat{x}, E) \hat{\sigma}(\hat{x}, y), \quad (4)$$

with f_g and f_u the parton distribution functions of the gluon and u type parton. Equations (3) and (4) define the W parton distribution function f_W .

In Eq.(4) we have replaced the W and gluon momenta, k and k' , by their z components. The approximation thus involves neglecting the transverse momenta in $\hat{\sigma}$, which is integrated over. Depending on whether one chooses to take $k^2 = 0$ or $k^2 = M_W^2$ for the W , this amounts to replacing the intermediate boson four momenta by $(\hat{x}E, 0, 0, \hat{x}E)$ or $(\hat{x}E, 0, 0, \sqrt{\hat{x}^2 E^2 - M_W^2})$, respectively. The integration over the transverse momenta is represented by the W parton distribution functions f_W . This will of course be a good approximation inasmuch as the process is strongly dominated by $k_T = 0$.

In passing from Eq.(3) to Eq.(4) one averages over the possible values of the transverse momenta. For ‘normal’ partons (the gluon, for instance) this leads to a mass singularity as $k_T \rightarrow 0$; the distribution is clearly peaked at low values of k_T , leading to the familiar logarithmic dependence on the scale. On the other hand, for the W the mass singularity is absent due to the mass in the propagator. There is thus a natural spread in the distribution of k_T which makes the effective- W approximation less accurate. Obviously the approximation becomes better the larger the value of E is. As we mentioned, Dawson[28] and others [29, 30] somehow estimated the accuracy of the approximation. Half the cross section for transverse W ’s comes from angles $\theta \leq \sqrt{M_W/2E}$, and the cross section is even more collimated for longitudinal W ’s. We have set a cut in the sub-process invariant mass to guarantee the validity of the effective- W approximation. If we neglect altogether the W mass, the invariant mass of the Wg system (or, for that matter, the top-anti-bottom system) is $4\hat{x}yEE_P$ (since the W and the gluon have opposite directions within this approximation). A lower cut in the invariant mass is a cut in \hat{x} , y and, in particular, on E . We shall in the following present results for a couple of cuts in the invariant mass, 500 GeV and 100 GeV. The validity of the effective- W approximation appears questionable in the second case, not so much in the first one. However one of our conclusions will be that no matter the cut that one sets in the invariant mass there are problems. The limiting factor will in fact be the LHC energy.

The upper limit for the integral over k_T sets the scale normalizing the (logarithmic) dependence on M_W of the structure functions. It is somewhat ambiguous to set a given value for this scale. Some authors (see e.g. [26, 31] take $k_T^{max} = E^2$ (the energy of the u or the gluon in its center-of-mass frame) while others take $4E^2$ [28]. It should be borne in mind that the uncertainty associated to using one value or another, while nominally subdominant

is again not so small at LHC energies, so the difference matters to some extent. The relevant expressions for f_W that we have used can be found in [28]. Next to leading calculations exist in the literature [30].

There are, in fact, two different parton distribution functions for the W , one for transverse and another one for longitudinal vector bosons, f_{W_T} and f_{W_L} respectively. Needless to say that the distinction between transverse and longitudinal W 's is not Lorentz invariant— a transverse photon may turn into a combination of transverse and longitudinal after a Lorentz transformation. However, provided that the changes of reference frame involve only boosts in the z direction, the transverse degrees of freedom remain transverse, while the longitudinal ones mix with the temporal ones, but gauge invariance of the physical amplitude for the sub-process does guarantee that the correct result is preserved. Since in the effective- W approximation all the dynamics in the initial state takes place in the z direction one needs not worry in which precise reference frame these distribution functions are defined.

It turns out to be absolutely crucial for our purposes to keep the parton distribution functions for the W as given, for instance in [28], without attempting to approximate them by assuming that $E \gg M_W$. For instance, one often finds in the literature the following approximate expression for f_{W_T}

$$f_{W_T}(\hat{x}) \simeq \frac{g^2}{(4\pi)^2} \frac{\hat{x}^2 + 2(1 - \hat{x})}{2\hat{x}} \log\left(\frac{4E^2}{M_W^2}\right), \quad (5)$$

Using this expression instead of the one given in [28] overestimates the total cross section by at least a factor five. To reach this conclusion we compare our results to our exact analytical calculation presented in [16]. When one looks in detail the kinematical regions that matter, the energy of the LHC is just not large enough to grant the approximation, and increasing the cut of 500 GeV in the sub-process invariant mass further does not really help. It is thus essential to use an expression for $f_{W_T}(\hat{x})$ which is valid over all ranges of \hat{x} . Even in this case the results are not fully satisfactory as we shall see in a moment.

Regarding the longitudinal W parton distribution function $f_{W_L}(\hat{x})$ we have realized that the complete expression given in [28] is incorrect because we have found numerically that it is not positive definite as it should. Despite of that we have found that the approximate expression (which is evidently positive definite) given in the same work

$$f_{W_L}(\hat{x}) \simeq \frac{g^2}{(4\pi)^2} \frac{1 - \hat{x}}{\hat{x}}, \quad (6)$$

gives rise to sensible results when compared to the ones obtained in the exact calculation. Because of that we have proceeded to use it, obtaining that the corresponding contribution to the final result is much smaller than the one coming from the transverse sector (about a 10 % in our case).

The fact that the longitudinal degrees of freedom should be subdominant can be understood on the following grounds. At large energies one can approximate the polarization vector ε_L^μ by k^μ/M_W . Taking into account that the longitudinal vector bosons couple to the light quarks, use of the equations of motion forces this term to vanish or be negligible. In fact, the only term that may survive is the one that is subdominant when one uses the above approximation for ε_L^μ , namely

$$\varepsilon_L^\mu = \frac{k^\mu}{M_W} + \frac{|\mathbf{k}| - k^0}{M_W} (1, 0, 0, -1), \quad (7)$$

We have used $\varepsilon_L^\mu = \frac{|\mathbf{k}| - k^0}{M_W} (1, 0, 0, -1)$ in all cases.

At this point one must commit oneself to a given choice for the k^2 of the virtual W as it is impossible to keep both the two light quarks and the W on shell. We have found, in fact, that for the final results it hardly matters whether one uses $k^2 = 0$ or $k^2 = M_W^2$ (or, presumably, anything in between). Here we shall present results of the latter option and we will postpone a more detailed discussion on this issue to another paper. The main argument in favour of this choice is that, except for the fact that one of the external legs is off-shell by an amount which is nevertheless small compared to the relevant energies, it is the one that matches smoothly the formulae for the W parton distribution functions given in [28]. In that case k^0 is always bigger than M_W and factors appearing in the W parton distribution functions of the form $(k^0 - M_W)^{-1/2}$ are well defined real numbers. If we want to take $k^2 = 0$ and use at the same time the results of [28] we have to impose an artificial cutoff enforcing $k^0 > M_W$ in order to assure a sensible cross section

The other obvious approximation involved in using the effective- W approximation is the neglect of the crossed interference term between longitudinal and transverse W 's. In the case at hand, the cross sections of the elementary subprocesses of Fig.1 are presented in the Appendix and it is not difficult to check that they are of the same order. However, the arguments we have given previously concerning the dominance of the transverse W make the longitudinal contribution subdominant. However, one should still worry about the interference term, which could easily give a correction of the order of 30 %. Fortunately it can be seen that integration over the azimuthal angle makes the interference term to approximately vanish[32, 30]. So in fact, the neglect of the interference term is not a bad approximation at all.

5 Cross Section for Single Top Production

We have thus proceeded as follows. We have multiplied the parton distribution function of a gluon of a given momenta from the first proton by the sum of parton distribution functions

for obtaining a u type quark from the second proton. Then we have multiplied this result by the probability of obtaining an on-shell transversal W^+ from those partons. We have repeated the process for a longitudinal vector boson. These results are then multiplied by the cross sections of the subprocesses of Fig.1 corresponding to transversal or longitudinal W^+ , respectively. At the end, these two partial results are add up to obtain the total $pp \rightarrow t\bar{b}$ cross section.

Since typically, the top quark decays weakly well before strong interactions become relevant, we can in principle measure its polarization state with virtually no contamination of strong interactions (see e.g. [11] for discussions on how this could be done). For this reason we have considered polarized cross sections and provide general formulas for the production of polarized tops in a general spin frame (within the context and limitations of the effective- W approximation). The mass of the b quark has been maintained all the way.

To calculate the event production rate corresponding to different observables and compare them with the theoretical predictions we have used the integrating montecarlo program VEGAS [33]. We present results after one year run at full luminosity in one detector (100 fb^{-1} at LHC). The scale used for α_s is the invariant mass of the partons (the gluon and the light quark). For the purposes of this work a more detailed study on this scale dependence does not seem necessary.

Let us start by discussing the experimental cuts. Due to geometrical detector constraints we adopt a pseudorapidity cut $|\eta| < 2.5$ both for the top and bottom. This corresponds to approximately 10 degrees from the z axis. As for p_T we have taken the cut $|p_T| > 30 \text{ GeV}$. Within the effective- W approximation the W and gluon transverse momenta are neglected; this implies that the top and bottom p_T are identical. This last assumption is not valid in an exact calculation and to what extent this changes the results depends on the cuts selected. We have also implemented an angular isolation cut for the top and anti-bottom (or anti-top and bottom) of 20 degrees. These cuts are relatively mild, they reduce the cross section by about a factor three.

In single top production a distinction is often made between $2 \rightarrow 2$ and $2 \rightarrow 3$ processes. The latter corresponds, in fact, to the process we have been discussing, the one represented in Fig.1, in which a gluon from the sea splits into a $b\bar{b}$ pair. In the $2 \rightarrow 2$ process the b quark is assumed to be extracted from the sea of the proton. Of course the distinction between the two processes is merely kinematical and somewhat arbitrary. In the remains of the proton a \bar{b} must be present, given that the proton has no net b content and thus the final state is also identical to the one we have been discussing. The values of the total cross sections presented in the introduction correspond to the kinematical cuts used in [10]. In the framework of our approximation all partons are deemed to have zero transverse momentum and hence the

detection of a \bar{b} in the fiducial zone, above the angular and/or p_T cuts, necessarily indicates that the \bar{b} originates from the ‘hard’ sub-process. In [16] we discuss this issue in more detail and a justification of the above signal for single top production is given. Let us just mention here that if we were to use the signal suggested by Willenbrock and coworkers (only one bottom tag in the final state) the effective- W approximation would be completely useless.

As for the cut in the invariant mass we have alluded to before, we have used two values, namely 500 GeV and 100 GeV. Both are somewhat extreme. The first one eliminates many events (the total cross section is reduced by an order of magnitude compared to the other cut), while the latter renders the effective- W approximation even more questionable. As we will see the comparison with the exact calculation does not really improve when the cut on the invariant mass is raised.

We shall start by considering the Standard Model tree-level predictions concerning single top production. In Table 2 and Figs. 3 and 4 we present our numerical results for production of polarized tops in the LAB helicity basis and compare them to an the exact calculation of the cross-section for the two cuts on the invariant mass. From these two figures we can see that the results obtained using the effective- W approximation differ significantly from the ones obtained from an exact calculation. In particular we immediately observe that the effective- W approximation systematically leads to many more left-handed tops than right-handed ones while the situation in an exact calculation is more complicated (we of course mean negative and positive helicity when we talk of left or right tops, chirality simply does not make sense for such a massive particle).

Indeed, the percentage of left tops with respect to the total production depends, in an exact calculation, critically on the cuts imposed. We have observed numerically in the exact calculation that left tops are produced in excess to right tops for low invariant mass and viceversa for high invariant mass. This is seems counterintuitive since we expect that at high invariant masses we could approximate the top as massless and therefore we expect it to be produced mainly left-handed polarized. However we have observed that in the particular mechanism considered for single top production in the LHC the average top energy is not much higher than its mass for such argument to hold. It is important to remark also that in order to compare the effective- W approximation results to the ones of an exact calculation no cuts are placed on the spectator quark in the last one (recall that the spectator quark is invisible in the effective- W approximation).

The fact that the effective- W approximation produces many more left tops than right ones can to some extent be understood on pure kinematical and angular momentum conservation arguments. Take for instance a relatively large cut in the invariant mass (such as 500 GeV). This automatically forces a back to back kinematics in the emerging top and anti-bottom

assumption	N_-	N_+
eff-W ($\sqrt{s} > 500$ GeV)	2.45×10^5	0.63×10^5
exact ($\sqrt{s} > 500$ GeV)	0.82×10^5	1.09×10^5
eff-W ($\sqrt{s} > 100$ GeV)	18.0×10^5	7.08×10^5
exact ($\sqrt{s} > 100$ GeV)	9.92×10^5	8.52×10^5

Table 2: Total number of events in single top production in the LAB helicity frame. We show a comparison between results obtained with and without the effective- W approximation in the tree level SM. Values calculated with $p_T > 30$ GeV., and $10^\circ < \theta < 170^\circ$. We present the comparison for invariant mass cuts of 500 and 100 GeV.

(see Fig.7). Since we know that the process is very much dominated by transverse W and the bulk of the processes take place in the forward direction, angular momentum conservation forces the top to emerge with a negative helicity. Indeed, the contribution of longitudinally polarized W 's does favour right handed tops, but it is numerically irrelevant (see Fig.5). The situation still persists at lower values of the invariant mass, where both back to back and same direction top-anti-bottom pairs are produced, but then the exact calculation also does give marginally more negatively polarized tops. Of course the above arguments do not really apply to the exact calculation, where the kinematics is a lot more involved.

We have also calculated single anti-top production. In Fig.6 we show two different histograms corresponding to the production of \bar{t} with the two possible helicities in the LAB frame and the 500 GeV cut on the invariant mass. All the histograms correspond to the tree level electroweak approximation and clearly show that single anti-top production is suppressed roughly by a factor of two with respect to single top production. This feature is general and is due to the different probability of extracting a W^- from a proton as compared to that of extracting a W^+ . The relevant electroweak cross sections (see Appendix) are symmetric under the interchange of particle by antiparticle along with helicity flip.

In Fig. 7 we plot the angular distribution of single top production in the (tree-level) Standard Model and compare them to the exact calculation [16] with an equivalent set of cuts. From the inspection of this figure we see that as expected the distribution is strongly peaked in the beam direction, with the probability of top and anti-bottom being produced back to back bigger than produced parallel. The exact calculation has similar features. The back to back production is favoured with respect to the parallel one due to the 500 GeV. cut in the invariant mass, as discussed. If we lower this cut in the exact calculation (the effective- W needs it) we observe that parallel configurations tend to equal or exceed back-to-back ones (see [16])

As we see, the predictions from the effective- W approximation coincides only roughly

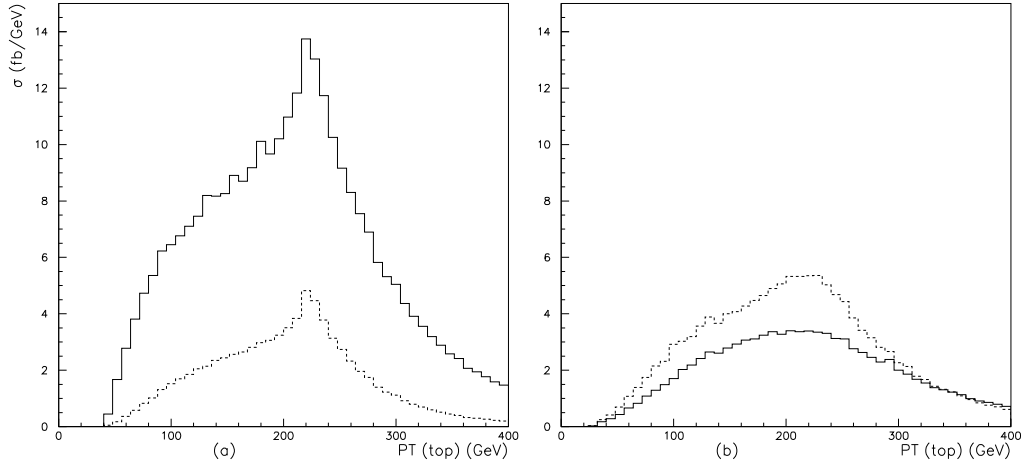


Figure 3: Differential cross section of (single) tops produced at the LHC vs. transversal momentum in the Standard Model. The solid (dotted) line corresponds to left (right) polarized top production. The subprocesses contributing to these histograms have been calculated at tree level in the electroweak theory with a cut of 500 GeV. in the top anti-bottom invariant mass. In the figure we show the results of the calculations for polarized top production in the LAB helicity basis. These predictions (a) are compared to those of the exact calculation (b). We see that the effective-W approximation fails to produce the correct polarization behaviour

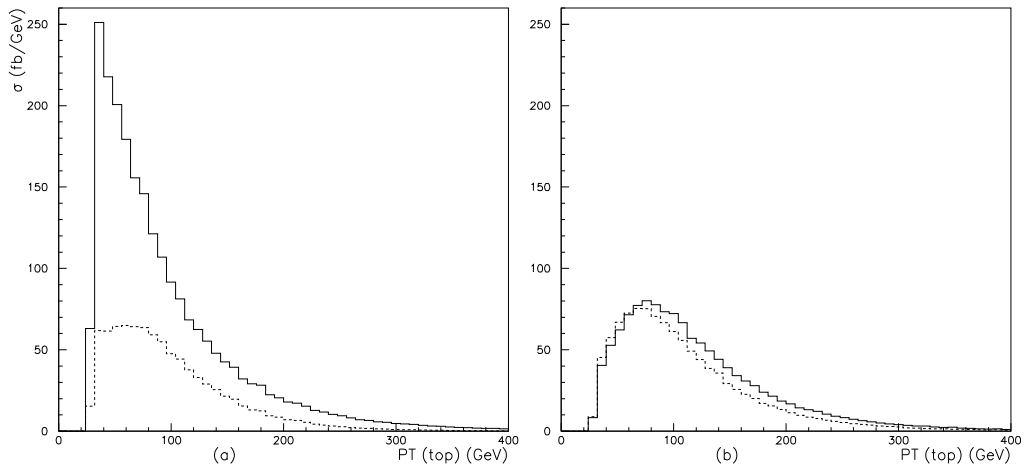


Figure 4: The same plots as in Fig.3 but with a cut of 100 GeV in the invariant mass of the top anti-bottom system. Again the effective-W approximation fails to account for the correct P_T distributions.

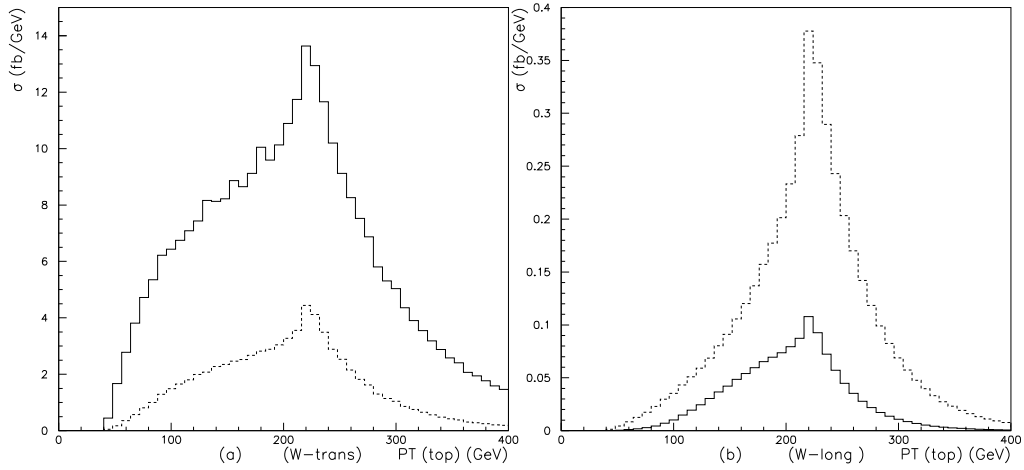


Figure 5: Differential cross section of (single) tops produced at the LHC vs. transversal momentum in the Standard Model. The solid (dotted) line corresponds to left (right) polarized top production. The subprocesses contributing to these histograms have been calculated at tree level in the electroweak theory with a cut of 500 GeV in the top anti-bottom invariant mass. In the figure we show the results of the calculations for polarized top production in the LAB helicity basis. Both figures are calculated in the effective- W approximation with (a), (b) showing the contribution coming from transverse and longitudinal polarized W respectively. It is clear that transverse W largely dominates (notice the different vertical scale).

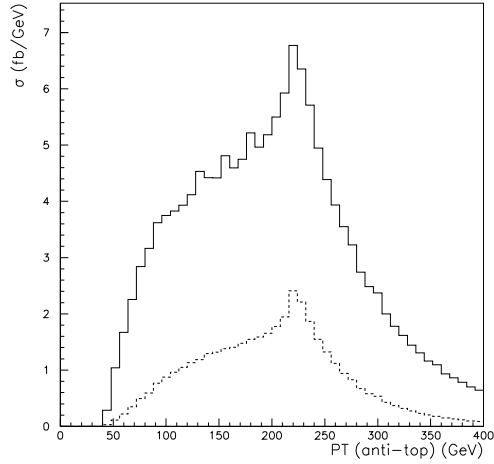


Figure 6: Differential cross section of (single) anti-top at the LHC vs. transversal momentum at tree level in the Standard Model. The solid (dotted) line corresponds to right (left) polarized anti-top production. Histograms correspond to subprocesses calculated in the tree level electroweak approximation in the LAB helicity frame within the effective- W approximation approach.

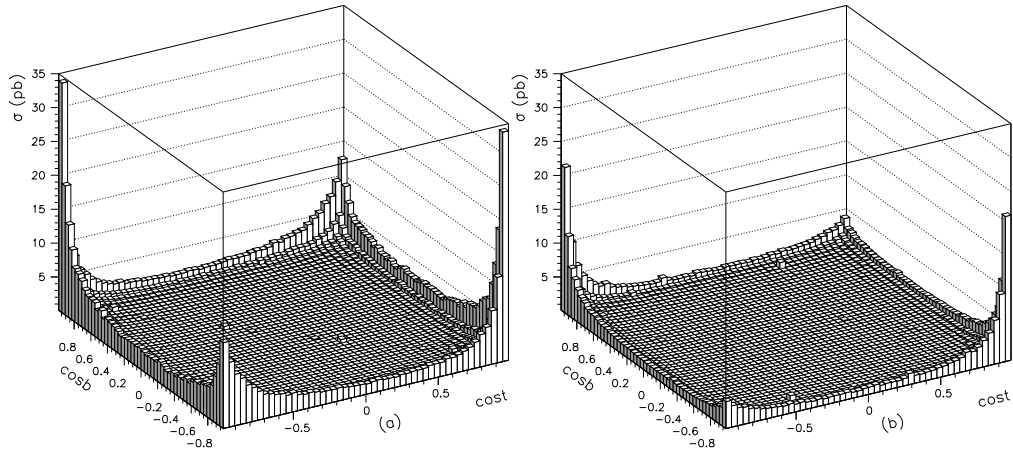


Figure 7: Expected angular distribution for single top production produced at the LHC in the Standard Model calculated in the effective W approximation (a) and with an exact calculation (b) .

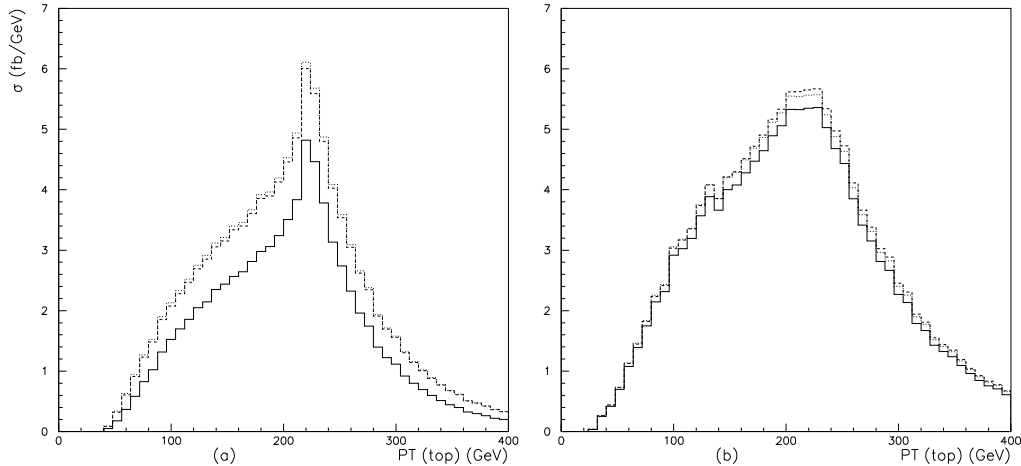


Figure 8: (a) Comparison between the tree Standard Model p_T distribution for single positively polarized top production (solid line) and the corresponding obtained with a value $g_R = \pm 0.3$ for the effective right handed coupling (dotted/dashed line) in the effective W approximation. (b) Same when the exact calculation is used.

with the exact calculation ones. The angular distribution is similar, and the total cross section is in the same ballpark, but this is about all. However, an intriguing feature of the approximation is that the production of positively polarized (right) tops comes out in surprising good agreement with the exact calculation. Indeed, let us now depart from the tree-level Standard Model and consider non-zero values for δg_R . In Fig. 8 we present a comparison between the effective- W approximation and the exact calculation for several values of the right effective couplings; the agreement is not bad. The cut for the invariant mass is 500 GeV. and the remaining cuts are the ones used so far.

6 Conclusions

We have done a complete calculation of the subprocess cross sections for polarized tops or anti-top production at the LHC including all mass corrections and with general effective couplings g_L and g_R . The calculations presented are fully analytical.

Then we have used those results to analyzed the single top production process at the LHC using the effective- W approximation. That is, considering that the W -boson is a real particle in order to calculate the probability of obtaining a W -boson from a proton as a product of probabilities. The effective- W approximation has in its favour its technical simplicity and a clear physical interpretation for those used to the language of parton distribution function,

being a generalization of the Weiszäcker-Williams approximation for photons, which works well.

In this work we have shown that the effective- W approximation is well suited for angular distributions and works reasonably well (but not exceedingly well) for total cross sections where it provides estimations that are in the same ballpark than those provided by an exact calculation. It fails however to reproduce the detailed p_T distributions. It does not reproduce well the fine details of the polarized top production, systematically giving far too many left tops. In summary, it is not really adequate for polarization studies and we urge the interested reader to use the methods discussed in [16].

7 Acknowledgments

It has been a pleasure to be able to present this work in the XXIX International Meeting on Fundamental Physics, in a special session devoted to the 60th birthday of Paco Ynduráin, to whom this work is dedicated, with our best wishes of a long and productive career. We would like to thank A.Dobado, M.J.Herrero, J.R.Peláez and E.Ruíz-Morales for multiple discussions. J.M. acknowledges a fellowship from Generalitat de Catalunya, grant 1998FI-00614. Financial support from grants AEN98-0431, 1998SGR 00026 and EURODAPHNE is greatly appreciated.

A Effective Couplings and Mixed States

Using our results (including the effective- W approximation) we obtain that the differential cross section matrix element at tree level can be written as

$$|M|^2 = \left(|g_R|^2 + |g_L|^2\right) a + \left(|g_R|^2 - |g_L|^2\right) b_n + m_b m_t \frac{g_R^* g_L + g_L^* g_R}{2} c \quad (8)$$

$$= \begin{pmatrix} g_R^* & g_L^* \end{pmatrix} \begin{pmatrix} a + b_n & \frac{m_b m_t}{2} c \\ \frac{m_b m_t}{2} c & a - b_n \end{pmatrix} \begin{pmatrix} g_R \\ g_L \end{pmatrix} \quad (9)$$

$$\equiv \begin{pmatrix} g_R^* & g_L^* \end{pmatrix} A \begin{pmatrix} g_R \\ g_L \end{pmatrix}, \quad (10)$$

where a , b_n , and c are independent of the effective couplings g_R and g_L and b_n is the only piece that depends on the top spin four-vector n . When $|M|^2$ corresponds to the matrix element of the subprocess the exact expressions for a , b_n , and c can be obtained from the formulae given in the Appendix B. For the matrix element of the whole process we have to multiply those expressions with the corresponding W and gluon parton distribution functions and make the sums over parton species and polarizations but all this respects the general form given in

Eq.(10). From Eq.(10) we can observe that CP violating phases appear suppressed by the bottom mass but at the same time they are enhanced by a g_L factor. Hence, if one manages to find a highly polarized spin basis there are some chances of having experimentally observable effects. This is for sure not the case in the LAB helicity basis as can be observed in Table 2. Also we see that to determine g_R we need to measure the top polarization.

Returning to the discussion of the general aspects of Eq.(10) we observe that A is a symmetric matrix and then it is diagonalizable. Moreover, from the positivity of $|M|^2$ we immediately arrive at the constraints

$$\det A = a^2 - b_n^2 - \frac{m_b^2 m_t^2 c^2}{4} \geq 0, \quad (11)$$

$$\frac{1}{2}TrA = a \geq 0. \quad (12)$$

In order to have a 100% polarized top we need a spin four-vector n that saturates constrain (11) for each kinematical situation, that is we need A to have a zero eigenvalue. In general such n need not exist and, should it exist, is in any case independent of the anomalous couplings g_R and g_L (this will not hold if we give up the effective- W approximation). Moreover, provided this n exists there is only one solution (up to a global complex normalization factor) for the pair (g_R, g_L) to the equation $|M|^2 = 0$, or equivalently to the eigenvector equation

$$A \begin{pmatrix} g_R \\ g_L \end{pmatrix} = 0, \quad (13)$$

To illustrate these considerations let us give an example: In the unphysical situation where $m_t \rightarrow 0$ it can be shown that there exists two solutions to the saturated constraint (11), namely

$$m_t n^\mu \rightarrow \pm \left(|\vec{p}_1|, p_1^0 \frac{\vec{p}_1}{|\vec{p}_1|} \right), \quad (14)$$

once we have found this result we plug it in the expression (13) and we find the solutions $(0, g_L)$ with g_L arbitrary for the + sign and $(g_R, 0)$ with g_R arbitrary for the - sign. That is, physically we have zero probability of producing a right handed top when we have only a left handed coupling and viceversa when we have only a right handed coupling. Note that if our theory had a massless top and whatever non-null anomalous couplings g_R and g_L then there would be no direction of 100% polarization. This can be understood remembering that the top particle forms in general an entangled state with the other particles of the process and since we are tracing over the unknown spin degrees of freedom of those particles we do not expect in general to end up with a top in a pure polarized state, although this is not impossible as it is shown the in above example.

B Subprocesses cross sections

In order to write the cross section of the subprocess, we define the spin four-vector corresponding to the spin in the \hat{n} direction as

$$n^\mu \equiv \frac{1}{\sqrt{(p_1^0)^2 - (\vec{p}_1 \cdot \hat{n})^2}} (\vec{p}_1 \cdot \hat{n}, p_1^0 \hat{n}),$$

with the properties

$$\begin{aligned} n^2 &= -1, \\ (n \cdot p_1) &= 0, \end{aligned}$$

which reduces in the case of \pm helicity ($\hat{n} = \pm \frac{\vec{p}_1}{|\vec{p}_1|}$) to

$$n^\mu \equiv \pm \frac{1}{m_t} \left(|\vec{p}_1|, p_1^0 \frac{\vec{p}_1}{|\vec{p}_1|} \right),$$

we have the differential cross section of the subprocess for single top production

$$\begin{aligned} d\sigma &= f_g(y) f_u(x) f_W(\hat{x}, E) dx dy d\hat{x} \delta^4(k_1 + k_2 - p_1 - p_2) \\ &\times \frac{1}{4 |k_2^0 \vec{k}_1 - k_1^0 \vec{k}_2|} \left(\prod_{f=1}^2 \frac{d^3 p_f}{(2\pi)^3 2E_f} \right) |M|^2 (2\pi)^4 \end{aligned}$$

and

$$|M|^2 = g_s^2 O_{ij} A_{ij} = g_s^2 (O_{11} A_{11} + O_{22} A_{22} + O_c (A_{12} + A_{21})),$$

where

$$\begin{aligned} O_{11} &= \frac{1}{4 (k_1 \cdot p_1)^2}, \\ O_{22} &= \frac{1}{4 (k_1 \cdot p_2)^2}, \\ O_c &= O_{12} = O_{21} = \frac{1}{4 (k_1 \cdot p_1) (k_1 \cdot p_2)}, \end{aligned}$$

and after averaging over gluon colours and transverse polarizations, and summing over fermion colours we have

$$\begin{aligned} A_{11} &= A_{11}^{(+)} + A_{11}^{(-)} + m_t m_b \varepsilon^2 \frac{g_R^* g_L + g_L^* g_R}{2} \{m_t^2 - k_1 \cdot p_1\} \\ &+ m_t^2 \left(|g_L|^2 + |g_R|^2 \right) \{2(\varepsilon \cdot p_2) (\varepsilon \cdot (k_1 - p_1)) - \varepsilon^2 (p_2 \cdot (k_1 - p_1))\}, \end{aligned}$$

with

$$\begin{aligned} A_{11}^{(\pm)} &\equiv |g_\pm|^2 \varepsilon \cdot p_2 \left\{ 2((k_1 - p_1) \cdot \varepsilon) \left((k_1 - p_1) \cdot \frac{p_1 \pm m_t n}{2} \right) - (k_1 - p_1)^2 \left(\varepsilon \cdot \frac{p_1 \pm m_t n}{2} \right) \right\} \\ &- |g_\pm|^2 \frac{\varepsilon^2}{2} \left\{ 2((k_1 - p_1) \cdot p_2) \left((k_1 - p_1) \cdot \frac{p_1 \pm m_t n}{2} \right) - (k_1 - p_1)^2 \left(p_2 \cdot \frac{p_1 \pm m_t n}{2} \right) \right\} \\ &+ |g_\pm|^2 \frac{m_t^2}{2} \left\{ 2(\varepsilon \cdot p_2) \left(\varepsilon \cdot \frac{p_1 \mp m_t n}{2} \right) - \varepsilon^2 \left(p_2 \cdot \frac{p_1 \mp m_t n}{2} \right) \right\}, \end{aligned}$$

and

$$A_{22} = A_{22}^{(+)} + A_{22}^{(-)} + m_b m_t \frac{g_R^* g_L + g_L^* g_R}{2} \{p_2 \cdot (p_2 - k_1)\} \varepsilon^2,$$

with

$$\begin{aligned} A_{22}^{(\pm)} \equiv & |g_{\pm}|^2 p_2 \cdot (k_2 - p_1) \left\{ 2(\varepsilon \cdot (k_2 - p_1)) \left(\varepsilon \cdot \frac{p_1 \pm m_t n}{2} \right) - \varepsilon^2 \left((k_2 - p_1) \cdot \frac{p_1 \pm m_t n}{2} \right) \right\} \\ & - \frac{|g_{\pm}|^2}{2} (k_2 - p_1)^2 \left\{ 2(\varepsilon \cdot p_2) \left(\varepsilon \cdot \frac{p_1 \pm m_t n}{2} \right) - \varepsilon^2 \left(p_2 \cdot \frac{p_1 \pm m_t n}{2} \right) \right\} \\ & + m_b^2 \frac{|g_{\pm}|^2}{2} \left\{ 2(\varepsilon \cdot (4k_1 - 3p_2)) \left(\varepsilon \cdot \frac{p_1 \pm m_t n}{2} \right) - \varepsilon^2 \left((4k_1 - 3p_2) \cdot \frac{p_1 \pm m_t n}{2} \right) \right\} \end{aligned}$$

and

$$\begin{aligned} A_{12} + A_{21} &= A_c^{(+)} + A_c^{(-)} \\ &\quad - m_b m_t \frac{g_R^* g_L + g_L^* g_R}{2} \left\{ \varepsilon^2 [2(p_2 \cdot p_1) - ((p_2 + p_1) \cdot k_1)] + 2(\varepsilon \cdot k_1)^2 \right\} \\ &\quad + \frac{|g_R|^2 + |g_L|^2}{2} \left\{ 2m_t^2 (\varepsilon \cdot p_2) (\varepsilon \cdot (k_2 - p_1)) - m_b^2 m_t^2 \varepsilon^2 \right\}, \end{aligned}$$

with

$$\begin{aligned} A_c^{(\pm)} &= 2|g_{\pm}|^2 (\varepsilon \cdot p_2) \left\{ \left((k_1 - p_1) \cdot \frac{p_1 \pm m_t n}{2} \right) (\varepsilon \cdot (k_2 - p_1)) \right. \\ &\quad \left. - \left(\frac{p_1 \pm m_t n}{2} \cdot (k_2 - p_1) \right) (k_1 \cdot \varepsilon) \right\} \\ &\quad - 2|g_{\pm}|^2 \left(\varepsilon \cdot \frac{p_1 \pm m_t n}{2} \right) \{ (\varepsilon \cdot p_2) (p_1 \cdot (k_1 - p_2)) \\ &\quad + (\varepsilon \cdot (k_2 - p_1)) ((k_1 - p_1) \cdot p_2) \\ &\quad - (\varepsilon \cdot (k_1 - p_1)) (p_2 \cdot (k_2 - p_1)) \} \\ &\quad + |g_{\pm}|^2 \varepsilon^2 \left\{ (p_2 \cdot (k_1 - p_1)) \left((k_2 - p_1) \cdot \frac{p_1 \pm m_t n}{2} \right) \right. \\ &\quad \left. + \left(p_2 \cdot \frac{p_1 \pm m_t n}{2} \right) ((k_2 - p_1) \cdot (k_1 - p_1)) \right. \\ &\quad \left. - (p_2 \cdot (k_2 - p_1)) \left((k_1 - p_1) \cdot \frac{p_1 \pm m_t n}{2} \right) \right\} \\ &\quad - 2|g_{\pm}|^2 m_b^2 (\varepsilon \cdot (k_1 - p_1)) \left(\varepsilon \cdot \frac{p_1 \pm m_t n}{2} \right), \end{aligned}$$

where ε is the polarization of the W^+ boson and

$$g_+ \equiv g_R,$$

$$g_- \equiv g_L,$$

For the subprocess of Fig.2 we have to perform the following changes in the expressions for the single top production.

$$\begin{aligned}
\varepsilon &\leftrightarrow \varepsilon^*, \\
n &\leftrightarrow -n, \\
p_2 &\leftrightarrow -p_2, \\
p_1 &\leftrightarrow -p_1, \\
k_2 &\leftrightarrow -k_2, \\
k_1 &\leftrightarrow -k_1,
\end{aligned}$$

but since we can take the W-boson polarization real and the cross section is even under the above sign changes, the subprocess cross section is the same for single top or anti-top production.

References

- [1] A.N. Okpara, hep-ph/0105151 and proceedings for the 36th Rencontres de Moriond, QCD and High Energy Hadronic Interactions, Les Arcs, France, March 17 - 24, (2001)
- [2] A.Dobado, D.Espriu and M.J.Herrero, Phys. Lett. B255 (1991) 405.
- [3] M. E. Peskin, J. D. Wells, hep-ph/0101342; M.S. Chanowitz, Phys.Rev. D59 073005 (1999) and hep-ph/0104024
- [4] T.Appelquist and C.Bernard, Phys. Rev. D22 (1980) 200; A.Longhitano, Phys. Rev. D22 (1980) 1166; A. Longhitano, Nucl. Phys. B188 (1981) 118; R.Renken and M.Peskin, Nucl. Phys. B211 (1983) 93; A.Dobado, D.Espriu and M.J.Herrero, Phys. Lett. B255 (1991) 405.
- [5] T.Appelquist, M.Bowick, E.Cohler and A.Hauser, Phys. Rev. D31 (1985) 1676.
- [6] See e.g. S.Catani, M.Mangano, P.Nason and L.Trentadue, Phys. Lett. B 378 (1996) 329
- [7] D. Espriu, J. Manzano, Phys.Rev.D63 (2001) 073008
- [8] T.M.P. Tait, Ph.D. Thesis, Michigan State University, 1999, hep-ph/9907462.
- [9] S.Dawson, Nucl. Phys. B249 (1985) 42; S.Willenbrock and D.Dicus, Phys. Rev. D34 (1986) 155; C.P.Yuan, Phys. Rev. D41 (1990) 42; R.K.Ellis and S.Parke, Phys. Rev. D46 (1992) 3785; G.Bordes and B. van Eijk, Z. Phys. C 57 (1993) 81, Nucl. Phys. B435

- (1995) 23; D.O.Carlson, Ph.D. Thesis, Michigan State University, 1995, hep-ph/9508278; T.Stelzer, Z.Sullivan and S.Willenbrock, Phys. Rev. D56 (1997) 5919.
- [10] T.Stelzer, Z.Sullivan and S.Willenbrock, Phys. Rev. D58 (1998) 094021
- [11] S.Parke, *Proceedings of the International Symposium on Large QCD Corrections and New Physics*, Hiroshima, 1997, Fermilab-Conf-97-431-T, hep-ph/9712512; G.Mahlon and S.Parke, Fermilab-Pub-99/361-T, hep-ph/9912458.
- [12] M. Fischer, S. Groote, J.G. Körner and M.C. Mauser, hep-ph/0101322
- [13] F.Larios and C.P.Yuan, Phys. Rev. D55 (1997) 7218.
- [14] Z.-H. Lin, T. Han, T. Huang, J.-X. Wang, X. Zhang, hep-ph/0106344
- [15] R. Peccei, X. Zhang, Nucl. Phys. B337 (1990) 269
- [16] D. Espriu, J. Manzano, hep-ph/0107112
- [17] T.Stelzer, Z.Sullivan and S.Willenbrock, Phys. Rev. D56 (1997) 5919
- [18] M.C. Smith, S. Willenbrock, Phys. Rev. D54 (1996) 6696
- [19] E.Bagan, D.Espriu, J.Manzano, Phys. Rev. D60, (1999) 114035.
- [20] T. Affolder et al (CDF collaboration) hep-ex/0012029
- [21] D.Amidei and C.Brock, *Report of the the TeV2000 study group on future electroweak physics at the Tevatron*, FERMILAB-PUB-96-082, 1996: S. Willenbrock, hep-ph/0103033
- [22] T.Swarnicki (for the CLEO collaboration), *Proceedings of the 1998 International Conference on HEP*, vol. 2, 1057.
- [23] F.Larios, M.A.Perez and C.P.Yuan, hep-ph/9903394; F.Larios, E.Malkawi, C.P.Yuan, Acta Phys. Polon. B27 (1996) 3741.
- [24] C.Weiszäcker and E.Williams, Z. Phys. 88 (1934) 244.
- [25] S.Frixione, M.Mangano, P.Nason and G.Ridolfi, Phys. Lett. B319 (1993) 339.
- [26] A. Dobado, M. J. Herrero, J. R. Pelaez, and E. Ruiz Morales, hep-ph/9912224
- [27] CTEQ4: H.-L. Lai et al., Phys. Rev. D55 (1997) 1280, <http://cteq.org>.
- [28] S. Dawson. Nucl.Phys. B249 (1985) 42-60.

- [29] G.L.Kane, W.W.Repko and W.B.Rolnick, Phys. Lett., 148B (1984) 367.
- [30] P.W.Johnson, F.J.Olness, and W.K.Tung, Phys. Rev. D36 (1987) 291.
- [31] B.Mele, in *Proceedings of the Workshop on Physics at Future Accelerators*, vol. II, p.13, J. Mulvey, ed. (1987).
- [32] J.Lindfors, Z. Phys. C28 (1985) 427; R.Kauffman, Ph. D. Thesis, SLAC-0348 (1989).
- [33] G.P.Lepage, Journal of Computational Physics 27 (1978) 192.